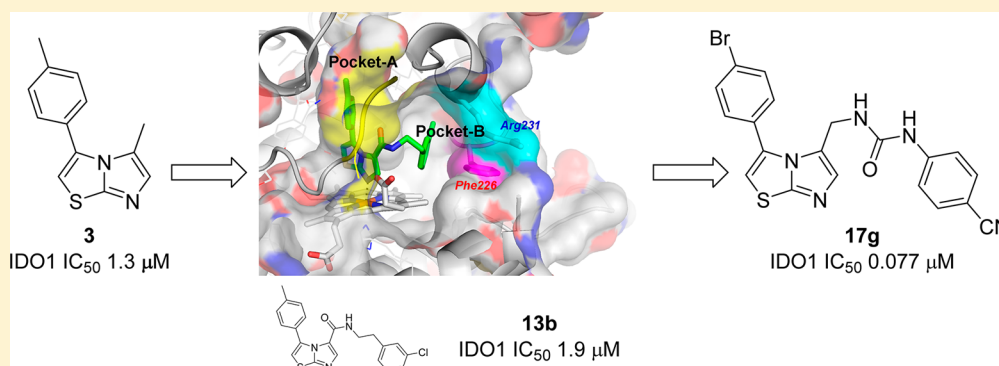


Crystal Structures and Structure–Activity Relationships of Imidazothiazole Derivatives as IDO1 Inhibitors

Shingo Tojo,^{*,†} Tetsuya Kohno,[†] Tomoyuki Tanaka, Seiji Kamioka, Yosuke Ota, Takayuki Ishii, Keiko Kamimoto, Shigehiro Asano, and Yoshiaki Isobe

Dainippon Sumitomo Pharma Co., Ltd., 3-1-98 Kasugade-naka, Konohana-ku, Osaka 554-0022, Japan

Supporting Information



ABSTRACT: Indoleamine 2,3-dioxygenase 1 (IDO1) is considered as a promising target for the treatment of several diseases, including neurological disorders and cancer. We report here the crystal structures of two IDO1/IDO1 inhibitor complexes, one of which shows that Amg-1 is directly bound to the heme iron of IDO1 with a clear induced fit. We also describe the identification and preliminary optimization of imidazothiazole derivatives as novel IDO1 inhibitors. Using our crystal structure information and structure–activity relationships (SAR) at the pocket-B of IDO1, we found a series of urea derivatives as potent IDO1 inhibitors and revealed that generation of an induced fit and the resulting interaction with Phe226 and Arg231 are essential for potent IDO1 inhibitory activity. The results of this study are very valuable for understanding the mechanism of IDO1 activation, which is very important for structure-based drug design (SBDD) to discover potent IDO1 inhibitors.

KEYWORDS: Indoleamine 2,3-dioxygenase 1, crystal structure, induced fit, structure-based drug discovery, imidazothiazole

X-ray crystallography is a powerful tool for clarifying target protein structures and plays a critical role in drug discovery, especially in structure-based drug design (SBDD), which is one of the most useful methods for lead generation and optimization. Detailed analysis of the crystal structure of a target protein/ligand complex is essential for SBDD and its success. Starting point of SBDD study is to obtain the suitable crystals of target protein/ligand complexes. However, the difficulty of it often depends on the target protein.¹ For example, heme-containing proteins present a challenge because preparation of highly active recombinant protein is very difficult.²

Indoleamine 2,3-dioxygenase 1 (IDO1) is a heme-containing protein that catalyzes the oxidative cleavage of the C2–C3 double bond of the indole in tryptophan to provide *N*-formyl-kynurenine. This reaction is known as the initial and rate-limiting step in the kynurenine pathway of tryptophan catabolism in mammals.^{3–6} The generated *N*-formyl-kynurenine is further metabolized to bioactive metabolites, including kynurenine, kynurenic acid, 3-hydroxy-kynurenine, and quinolinic acid, which are known to be involved in a number of neurological disorders, such as Alzheimer's disease, Parkinson's

disease, and cerebral ischemia.⁷ In addition, overexpression of IDO1 has been reported in many tumor cells,⁸ and IDO1 is considered as one of the key factors that contributes to cancer immunosuppression in tumor microenvironment. IDO1 helps create a tolerogenic state in both the tumor and its draining lymph nodes by both direct suppression of T cells and enhancement of local regulatory T cells.⁹ As IDO1 is strongly induced by interferon γ , which is produced by cytotoxic T lymphocytes,¹⁰ it presumably impairs the antitumor efficacy of other immune therapy. Therefore, inhibition of IDO1 would be very useful for the treatment of not only neurological diseases but also cancer.

To date, several types of IDO1 inhibitors, including tryptophan derivatives as represented by 1-methyltryptophan (1-MT),¹¹ 4-phenyl imidazole (PI) analogues,^{12,13} the thiazolotriazole compound Amg-1,¹⁴ and the hydroxylamide compound **1**,¹⁵ have been reported (Figure 1). Compound **1** has the most potent IDO1 inhibitory activity ($IC_{50} = 67$ nM, ref

Received: June 10, 2014

Accepted: August 19, 2014

Published: August 21, 2014



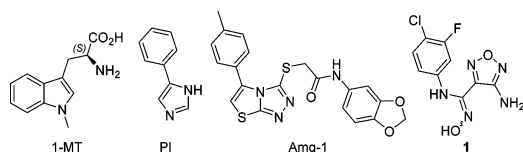


Figure 1. Structures of representative IDO1 inhibitors.

15) in currently reported IDO1 inhibitors. Even though a number of IDO1 inhibitors have been reported, only the crystal structure of IDO1/PI complex is currently available.¹⁶ This indicates that preparation of suitable crystals of IDO1/IDO1 inhibitor complex would be very difficult, probably due to additional technical issues distinctive of IDO1 as a heme-containing protein.²

It is reported that PI interacts directly with IDO1 heme iron at the imidazole nitrogen and that its phenyl group fits deeply into one of IDO1 hydrophobic pockets (pocket-A). The other hydrophobic pocket (pocket-B) is occupied by two molecules of the buffer *N*-cyclohexyl-2-aminoethanesulfonic acid (CHES) (Figure 2a; and the stereoview, see Figure S1 in the Supporting

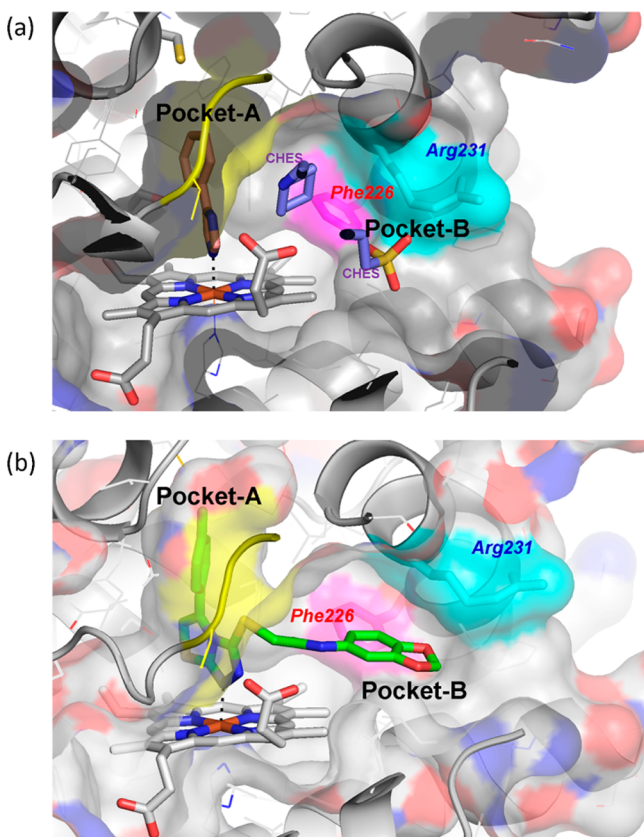


Figure 2. (a) Crystal structure of IDO1/PI (purple) complex (PDB: 2DOT). CHES is colored in blue. (b) Crystal structure of IDO1/Amg-1 (green) complex (PDB: 4PK5). Main chain Ala260-Ser263 (yellow), Phe226 (pink), and Arg231 (cyan) are shown in both panels.

Information). According to Shiro et al.,¹⁶ site-direct mutagenesis analysis of IDO1 catalytic activity is ensured by two amino acid residues: Phe226 and Arg231, both of which are part of the residues forming pocket-B. They hypothesized that both residues are directly involved in substrate recognition by hydrophobic interactions.

Almost all studies of IDO1 inhibitors make use of the crystal structure information on IDO1/PI complex or related plausible docking models to optimize their compounds. However, many of these studies discuss only the structure–activity relationships (SAR) at the pocket-A and the interaction with the heme iron without addressing SAR at the pocket-B. The reason should be that PI is a fragment-like inhibitor and interacts directly with heme iron and pocket-A, not pocket-B.

In our discovery study for novel IDO1 inhibitors, we considered that crystal structure information on IDO1/IDO1 inhibitor complex at pocket-B and elucidation of SAR at pocket-B are important for finding potent IDO1 inhibitors. Herein we report crystal structures of two IDO1/IDO1 inhibitor complexes, where the inhibitor interacts directly with pocket-B. We also describe the identification and SAR of a series of imidazothiazole derivatives as novel IDO1 inhibitors.

First, we sought to obtain the crystal structure of IDO1/IDO1 inhibitor complex. For that, we initially prepared a highly homogeneous recombinant IDO1 protein with a heme content ratio of approximately 78% compared to fully native heme-incorporated IDO1 protein.¹⁴ Incubation in 0.75 mM δ -aminolaevulinic acid at 30 °C for 12 h and purification with a strong reductant buffer containing 1 mM tris(2-carboxyethyl)-phosphine (TCEP) were essential in achieving a heme content ratio of more than 70%. Next, we turned our attention to crystallization of IDO1/IDO1 inhibitor complex. Here, adding the inhibitor while removing TCEP using a desalting column was very important for crystallization. Investigation of some currently reported IDO1 inhibitors led to the crystal structure of IDO1/Amg-1 complex as shown in Figure 2b (for the omit map and the stereoview, see Figure S2a,b in the Supporting Information). Interestingly, contrary to a previous report,¹⁴ which suggests that Amg-1 does not interact with heme iron, we found that the nitrogen of thiazolo-triazole in Amg-1 was directly bound to the heme iron and that tolyl group was placed at pocket-A. Furthermore, IDO1/Amg-1 complex showed a remarkable induced fit compared to IDO1/PI complex. Pocket-A expanded as structure of the main chain Ala260-Ser263 changed, and a shift of both Phe226 and Arg231 resulted in extension of pocket-B. The amide side chain of Amg-1 located at the expanded pocket-B, and the methylenedioxyphenyl moiety took a position adjacent to both residues. These findings were considered as encouraging for SBDD since they provided, for the first time, an induced fit for the crystal structure of IDO1/IDO1 complex and allowed acquisition of precise structure information, where IDO1 inhibitor directly interacted with IDO1 protein at both pocket-A and pocket-B.

To confirm the potential of the basic scaffold of Amg-1, we evaluated IDO1 inhibitory activity of the *para*-tolyl thiazolo-triazole compound 2. Like PI, compound 2 showed weak IDO1 inhibitory activity (Figure 3). The crystal structures of Amg-1 and PI revealed that both 2 and PI would bind to IDO1 at the same site and that 2 would directly interact with the heme iron. We focused on the pK_a value of the nitrogen atom bound to the heme iron to design a novel IDO1 inhibitor since compound 2 calculated pK_a value (1.09) was significantly lower than that of PI (6.56). As it is generally known that the basicity of a ligand is very important for forming a metal complex, we assumed that it would be possible to improve IDO1 inhibitory activity of 2 by control of the basicity of the nitrogen atom. Namely, we thought that strong basicity of nitrogen atom would result in strong binding to heme iron of IDO1; consequently, such compound should have potent IDO1 inhibitory activity. Hence,

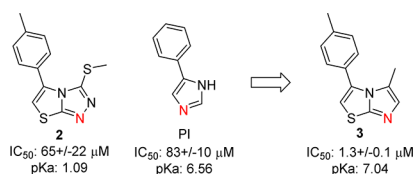
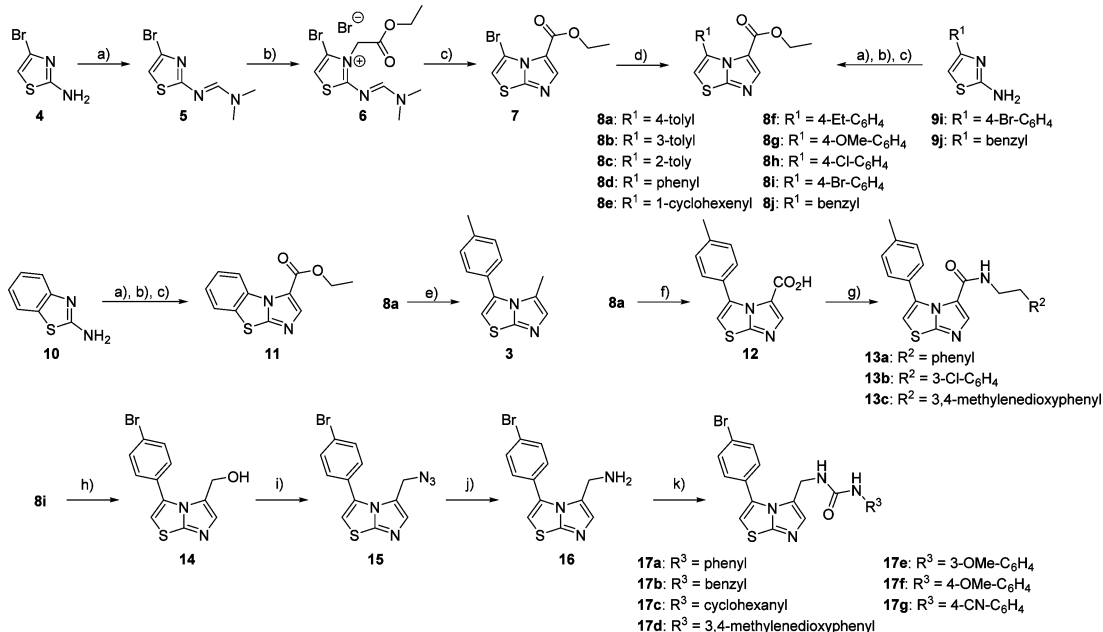


Figure 3. Design of the new imidazothiazole scaffold based on **2** and PI pK_a values. The nitrogen atom that binds to the heme iron is highlighted in red. IC_{50} values are the mean of at least two independent assays. pK_a values were calculated by ACD/Laboratories ver. 11.0.

we designed the *para*-tolyl imidazothiazole compound **3** as a novel scaffold by combining **2** and PI. The calculated pK_a value of the corresponding nitrogen atom of **3** was 7.04, which is similar to the basicity of PI. As predicted, IDO1 inhibitory activity of **3** was more potent than that of **2**. These findings indicated that **3** is a good starting compound for our discovery study.

The imidazothiazole derivatives were prepared by the following sequence (Scheme 1). First, the imidazothiazole scaffold was constructed in 3 steps as previously described¹⁷ with some modifications. Treatment of the 4-bromothiazol-2-amine **4** with *N,N*-dimethylformamide dimethyl acetal gave the amidine compound **5**. Salt formation in ethyl bromoacetate and subsequent treatment of the salt **6** with DBU afforded the imidazothiazole compound **7**. Suzuki couplings¹⁸ with boronic acids or pinacol boronates proceeded smoothly to provide 3-substituted imidazothiazole derivatives **8a–h**. The bromine compound **8i**, benzyl compound **8j**, and fused ring derivative **11**¹⁷ were prepared from the corresponding thiazol-2-amine **9i–j** and **10** by a similar method. Reduction of the ethyl ester **8a** with $LiAlH_4$ and $AlCl_3$ gave the methyl compound **3**. The amide derivatives **13a–c** were readily prepared in 2 steps.

Scheme 1. Synthesis of the Imidazothiazole Compounds^a



^aReagents and conditions: (a) *N,N*-dimethylformamide dimethyl acetal, DMF, 80 °C; (b) ethyl bromoacetate, 80 °C; (c) DBU, DMF, 60 °C; (d) $R^1B(OH)_2$ or R^1BPin , $Pd(PPh_3)_4$, K_2CO_3 , 1,4-dioxane- H_2O (3:1), 100 °C; (e) $LiAlH_4$, $AlCl_3$, THF, reflux (15%); (f) 1 N NaOH, MeOH-THF (99%); (g) $R^2CH_2CH_2NH_2$, WSC-HCl, HOBT, *i*-Pr₂NEt, DMF; (h) DIBAL-H, THF, 0 °C (94%); (i) DPPA, DBU, DMF, 60 °C (75%); (j) PPh₃, H_2O , THF, 45 °C (90%); (k) R^3NCO , *i*-Pr₂NEt, THF.

Hydrolysis of the ethyl ester **8a** to give the carboxylic acid **12** and subsequent amide formation reaction with $R^2CH_2CH_2NH_2$ and WSC-HCl gave the amide compounds **13a–c**. The urea derivatives **17a–g** were easily prepared in 4 steps from **8i**. Reduction of the ethyl ester **8i** with DIBAL-H afforded the alcohol **14** in 94%. The alcohol group of **14** was then converted with DPPA and DBU¹⁹ to the azide compound **15**, which was reduced under Staudinger conditions²⁰ to provide the amine compound **16**. Finally, treatment of **16** with isocyanate gave the urea compounds **17a–g**.

To improve IDO1 inhibitory activity, we first examined a way to optimize pocket-A using ethyl ester derivatives. As shown in Table 1, the *para*-tolyl compound **8a** was preferable to the

Table 1. IDO1 Inhibitory Activity of the Ethyl Ester Derivatives **8a–j** and **11**

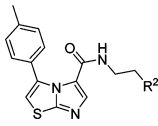
compd	R^1	IDO1 IC_{50} (μM) ^a
8a	4-tolyl	18 ± 3.7
8b	3-tolyl	>100
8c	2-tolyl	>100
8d	phenyl	>100
8e	1-cyclohexenyl	>100
8f	4-Et-C ₆ H ₄	24 ± 4.0
8g	4-MeO-C ₆ H ₄	56 ± 2.0
8h	4-Cl-C ₆ H ₄	8.1 ± 1.7
8i	4-Br-C ₆ H ₄	5.5 ± 2.2
8j	benzyl	>100
11		>100

^a IC_{50} values are the mean of at least two independent assays.

meta-tolyl compound **8b** or the *ortho*-tolyl compound **8c**, while the nonsubstituted phenyl compound **8d** and the 1-cyclohexene compound **8e** were not effective. IDO1 inhibitory activity of the ethyl compound **8f** and the methoxy compound **8g** was less than that of **8a**. Fortunately, introduction of a halogen atom onto the *para*-position was favorable, allowing both the chlorine compound **8h** and the bromine compound **8i** to be more effective than the *para*-tolyl compound **8a**. Both the benzyl compound **8j** and the fused ring type compound **11** were inactive.

Next, we attempted to optimize pocket-B by converting the ester moiety of **8a** and prepared the amide derivatives (**13a**, **13b**, and **13c**), which have a side chain the same length as that of Amg-1 (Table 2). However, these compounds showed

Table 2. IDO1 Inhibitory Activity of the Amide Derivatives **13a–c**



compd	R ²	IDO1 IC ₅₀ (μM) ^a
13a	phenyl	3.5 ± 1.0
13b	3-Cl-C ₆ H ₄	1.9 ± 0.5
13c	3,4-methylenedioxyphenyl	3.6 ± 1.2

^aIC₅₀ values are the mean of at least two independent assays.

almost the same IDO1 inhibitory activity as Amg-1 (IC₅₀ = 3.0 μM, ref 14), even though their basic scaffold had a potential superior to that of Amg-1. We therefore suspected that the side chain of these compounds in pocket-B should not be located exactly at the same position as the side chain of Amg-1. In fact, the crystal structure of IDO1/**13b** complex supported this hypothesis (Figure 4; for the omit map and the stereoview, see

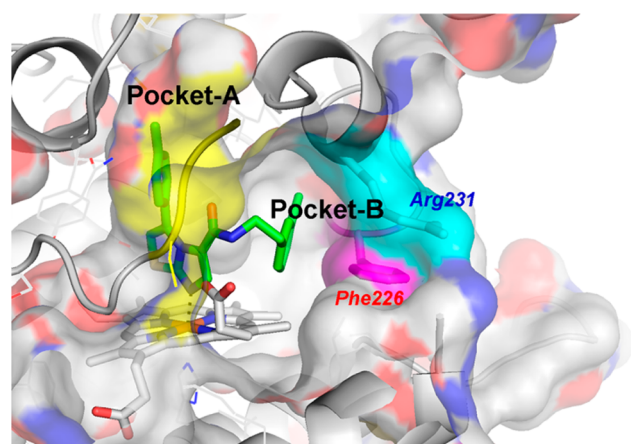


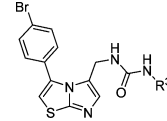
Figure 4. Crystal structure of IDO1/**13b** complex (green) (PDB: 4PK6). Main chain Ala260-Ser263 (yellow), Phe226 (pink), and Arg231 (cyan) are shown.

Figure S3a,b in the Supporting Information). The nitrogen of imidazothiazole in **13b** was directly bound to the heme iron and that tolyl group located at the expanded pocket-A in the same manner as Amg-1. However, the side chain of **13b** was bent sharply at the methylene moiety since the shape of pocket-B was dramatically changed by the shift of Phe226.

Consequently, **13b** generated an induced fit and located adjacent to Phe226, but not to Arg231.

These results indicated that as in Amg-1, a linearly rigid linker had to be introduced into the side chain to allow interaction with both the Phe226 and Arg231. Hence, we designed to introduce a urea group as a linearly planar unit into the linker moiety (Table 3). Introduction of the urea unit

Table 3. IDO1 Inhibitory Activity of the Urea Derivatives **17a–g**



compd	R ³	IDO1 IC ₅₀ (μM) ^a
17a	phenyl	0.22 ± 0.03
17b	benzyl	0.75 ± 0.01
17c	cyclohexanyl	1.8 ± 0.40
17d	3,4-methylenedioxyphenyl	0.12 ± 0.04
17e	3-MeO-C ₆ H ₄	0.16 ± 0.03
17f	4-MeO-C ₆ H ₄	0.19 ± 0.05
17g	4-CN-C ₆ H ₄	0.077 ± 0.015

^aIC₅₀ values are the mean of at least two independent assays.

predictably improved IDO1 inhibitory activity in a large number of derivatives (**17a**, **17d**, **17e**, **17f**, and **17g**) with the same length of side chain as Amg-1. The benzyl compound **17b** was less effective than the phenyl compound **17a**, which showed that the length of the linker is very important for an adjacent location to Phe226 and Arg231. IDO1 inhibitory activity of the cyclohexane compound **17c** was much lower than that of the phenyl compound **17a**. This suggested that the phenyl group interacts with Phe226 by a π - π interaction not a hydrophobic interaction (Figure 5). Furthermore, the *meta*-

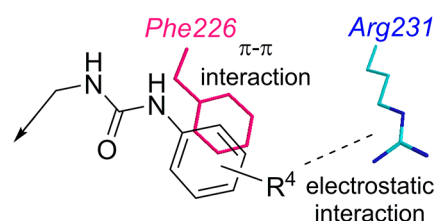


Figure 5. Plausible interactions of urea derivatives with Phe226 (pink) and Arg231 (cyan).

and/or *para*-substituted compounds (**17d**, **17e**, **17f**, and **17g**) were more effective than the unsubstituted compound **17a**. Particularly, the nitrile compound **17g** was the most effective compound with an IDO1 inhibitory activity comparable to that of **1**. These SARs support the idea that electrostatic interaction of Arg231 with a functional group substituted at the *meta*- and/or *para*-position of the phenyl group is necessary for potent IDO1 inhibitory activity. These results demonstrate that induced fit by extension of pocket-B and resulting interaction with both Phe226 and Arg231 would be essential for potent IDO1 inhibitory activity and are in accord with the results of previous site-direct mutagenesis analysis.¹⁶ Furthermore, this is the first case that clarified in detail the SAR at pocket-B.

In summary, to find novel potent IDO1 inhibitors, we determined the crystal structures of two IDO1/IDO1 inhibitor complexes, one of which showed that Amg-1 is directly bound

to the heme iron of IDO1 with a clear induced fit. Using this information, we identified the *para*-tolyl imidazothiazole compound **3** as a novel IDO1 inhibitor. Additionally, on the basis of crystal structure information on IDO1/**13b** complex, we found a series of urea derivatives as potent IDO1 inhibitors. Our novel structure information and SAR at the pocket-B revealed that generation of an induced fit and the resulting interaction with Phe226 and Arg231 are essential for potent IDO1 inhibitory activity. We believe that this study is very important for understanding the mechanism of IDO1 activation, which is very important for SBDD to find potent IDO1 inhibitors. Further efforts to discover a promising candidate are in progress.

■ ASSOCIATED CONTENT

Supporting Information

Supplementary figures, synthetic procedures, characterization, purification method of recombinant IDO1 protein, biological assays, and X-ray crystallography. This material is available free of charge via the Internet at <http://pubs.acs.org>.

■ AUTHOR INFORMATION

Corresponding Author

*(S.T.) Phone: +81-6-6466-5193. Fax: +81-6-6466-5297. E-mail: shingo-tojo@ds-pharma.co.jp.

Author Contributions

†S.T. and T.K. contributed equally to this study. S.T. directed medicinal chemistry. T.K. directed purification of IDO protein and X-ray crystallography.

Notes

The authors declare no competing financial interest.

■ ACKNOWLEDGMENTS

We are deeply grateful to Prof. Y. Shiro (RIKEN Harima Institute/Spring-8 Japan) for his fruitful discussion and advice. We also thank Ms. E. Koga and Dr. K. Kubota for their helpful discussion, Ms. S. Sasabe for collecting data on biological assays, and Ms. K. Yokokawa for her synthetic technical assistance.

■ ABBREVIATIONS

WSC, 1-ethyl-3-(3'-dimethylaminopropyl)carbodiimide; HOBt, 1-hydroxybenzotriazole; DIBAL-H, diisobutylaluminum hydride; DPPA, diphenylphosphoryl azide; DBU, 1,8-diazabicyclo[5.4.0]undec-7-ene

■ REFERENCES

- (1) Grey, J.; Thompson, D. Challenges and opportunities for new protein crystallization strategies in structure-based drug design. *Expert Opin. Drug Discovery* **2010**, *5*, 1039–1045.
- (2) Jung, Y.; Kwak, J.; Lee, Y. High-level production of heme-containing holoproteins in *Escherichia coli*. *Appl. Microbiol. Biotechnol.* **2001**, *55*, 187–191.
- (3) Takikawa, O.; Yoshida, R.; Kido, R.; Hayaishi, O. Tryptophan degradation in mice initiated by indoleamine 2,3-dioxygenase. *J. Biol. Chem.* **1986**, *261*, 3648–3653.
- (4) Takikawa, O. Biochemical and medical aspects of the indoleamine 2,3-dioxygenase initiated L-tryptophan metabolism. *Biochem. Biophys. Res. Commun.* **2005**, *338*, 12–19.
- (5) Efimov, I.; Basran, J.; Thackray, S. J.; Handa, S.; Mowat, C. G.; Raven, E. L. Structure and reaction mechanism in heme dioxygenases. *Biochemistry* **2011**, *50*, 2717–2724.

- (6) Forouhar, F.; Anderson, R. J. L.; Mowat, C. G.; Vorobiev, S. M.; Hussain, A.; Abashidze, M.; Bruckmann, C.; Thackray, S. J.; Seetharaman, J.; Tucker, T.; Xiao, R.; Ma, L.; Zhao, L.; Acton, T. B.; Montelione, G. T.; Chapman, S. K.; Tong, L. Molecular insights into substrate recognition and catalysis by tryptophan 2,3-dioxygenase. *Proc. Natl. Acad. Sci. U.S.A.* **2007**, *104*, 473–478.

- (7) Vécsei, L.; Szalárdy, L.; Fülöp, F.; Toldi, J. Kynurenes in the CNS: recent advances and new questions. *Nat. Rev. Drug Discovery* **2013**, *12*, 64–82.

- (8) Godin-Ethier, J.; Hanafi, L.; Piccirillo, C. A.; Lapointe, R. Indoleamine 2,3-dioxygenase expression in human cancers: Clinical and Immunologic perspectives. *Clin. Cancer Res.* **2011**, *17*, 6985–6991.

- (9) Munn, D. H.; Mellor, A. L. Indoleamine 2,3-dioxygenase and tumor-induced tolerance. *J. Clin. Invest.* **2007**, *117*, 1147–1154.

- (10) Katz, J. B.; Muller, A. J.; Prendergast, G. C. Indoleamine 2,3-dioxygenase in T-cell tolerance and tumoral immune escape. *Immunol. Rev.* **2008**, *222*, 206–221.

- (11) Cady, S. G.; Sono, M. 1-Methyl-DL-tryptophan, beta-(3-benzofuranyl)-DL-alanine (the oxygen analog of tryptophan), and beta-[3-benzo(b)-thienyl]-DL-alanine (the sulfur analog of tryptophan) are competitive inhibitors for indoleamine 2,3-dioxygenase. *Arch. Biochem. Biophys.* **1991**, *291*, 326–333.

- (12) Kumar, S.; Jaller, D.; Patel, B.; LaLonde, J. M.; DuHadaway, J. B.; Malachowski, W. P.; Prendergast, G. C.; Muller, A. J. Structure based development of phenylimidazole-derived inhibitors of indoleamine 2,3-dioxygenase. *J. Med. Chem.* **2008**, *51*, 4968–4977.

- (13) Röhrig, U. F.; Majjigapu, S. R.; Grosdidier, A.; Bron, S.; Stroobant, V.; Pilotte, L.; Colau, D.; Vogel, P.; Van den Eynde, B. J.; Zoete, V.; Michielin, O. Rational design of 4-aryl-1,2,3-triazoles for indoleamine 2,3-dioxygenase 1 inhibition. *J. Med. Chem.* **2010**, *53*, 1172–1189.

- (14) Meininger, D.; Zalameda, L.; Liu, Y.; Stepan, L. P.; Borges, L.; McCarter, J. D.; Sutherland, C. L. Purification and kinetic characterization of human indoleamine 2,3-dioxygenases 1 and 2 (IDO1 and IDO2) and discovery of selective IDO1 inhibitors. *Biochim. Biophys. Acta* **2011**, *1814*, 1947–1954.

- (15) Yue, E. W.; Douty, B.; Wayland, B.; Bower, M.; Liu, X.; Leffet, L.; Wang, Q.; Bowman, K. J.; Hansbury, M. J.; Liu, C.; Wei, M.; Li, Y.; Wynn, R.; Burn, T. C.; Koblisch, H. K.; Fridman, J. S.; Metcalf, B.; Scherle, P. A.; Combs, A. P. Discovery of potent competitive inhibitors of indoleamine 2,3-dioxygenase with in vivo pharmacodynamic activity and efficacy in a mouse melanoma model. *J. Med. Chem.* **2009**, *52*, 7364–7367.

- (16) Sugimoto, H.; Oda, S.; Otsuki, T.; Hino, T.; Yoshida, T.; Shiro, Y. Crystal structure of human indoleamine 2,3-dioxygenase: Catalytic mechanism of O₂ incorporation by a heme-containing dioxygenase. *Proc. Natl. Acad. Sci. U.S.A.* **2006**, *103*, 2611–2616 The crystal structure of IDO1/cyanid complex is also reported in this letter. However, we recognize cyanid as purely a ligand of heme iron.

- (17) Landreau, C.; Deniaud, D.; Evain, M.; Reliquet, A.; Meslin, J. C. Efficient regioselective synthesis of triheterocyclic compounds: imidazo[2,1-*b*]benzothiazoles, pyrimido[2,1-*b*]benzothiazolones and pyrimido[2,1-*b*]benzothiazoles. *J. Chem. Soc., Perkin Trans. 1* **2002**, 741–745.

- (18) Miyaura, N.; Yamada, K.; Suzuki, A. A new stereospecific cross-coupling by the palladium-catalyzed reaction of 1-alkenylboranes with 1-alkenyl or 1-alkynyl halides. *Tetrahedron Lett.* **1979**, *36*, 3437.

- (19) Thompson, A. S.; Humphrey, G. R.; DeMarco, A. M.; Mathre, D. J.; Grabowski, E. J. J. Direct conversion of activated alcohols to azides using diphenyl phosphorazidate. A practical alternative to Mitsunobu conditions. *J. Org. Chem.* **1993**, *58*, 5886–5888.

- (20) Staudinger, H.; Meyer, J. Über neue organische phosphorverbindungen III. Phosphinmethylenderivate und phosphinimine. *Helv. Chim. Acta* **1919**, *2*, 635–646.